AIMS Materials Science, 4(3): 814-831.
DOI: 10.3934/matersci.2017.3.814
Received: 09 May 2017
Accepted: 29 June 2017
Published: 03 July 2017

http://www.aimspress.com/journal/Materials

Research article

Physical and thermo-mechanical properties of bionano reinforced poly(butylene adipate-co-terephthalate), hemp/CNF/Ag-NPs composites

Harikrishnan Pulikkalparambil [1], Jyotishkumar Parameswaranpillai [1,3], Jinu Jacob George [1], Krittirash Yorseng [2], and Suchart Siengchin [2,3,4,*]

[1] Department of Polymer Science and Rubber Technology, Cochin University of Science and Technology (CUSAT), Kochi, Kerala, India
[2] Department of Mechanical and Process Engineering, The Sirindhorn International Thai-German Graduate School of Engineering (TGGS), King Mongkut's University of Technology North Bangkok, Bangkok, Thailand
[3] Center of Innovation in Design and Engineering for Manufacturing, King Mongkut's University of Technology North Bangkok, Bangkok, Thailand
[4] Natural Composite Research Group, King Mongkut's University of Technology North Bangkok, Bangkok, Thailand

* **Correspondence:** Email: suchart.s.pe@tggs-bangkok.org.

Abstract: A facile approach to prepare bionanocomposites of poly(butylene adipate-co-terephthalate) (PBAT) is reported in this paper. The effect of different wt% of hemp/Sihemp, carbon nanofiber (CNF) and silver nanoparticle (Ag-NPs) on the density, water absorption, melting and crystallization behavior, thermal stability, mechanical properties and morphology was investigated. The density of the composites was reduced except for Ag-NPs reinforced nanocomposites while diffusion coefficient and maximum water absorption were decreased for Sihemp reinforced composites making it a suitable material to replace conventional polymers. Significant improvement in tensile strength (TS) and tensile modulus (TM) was observed for the PBAT/Sihemp composites. For CNF and Ag-NPs reinforced nanocomposites, mechanical properties were retained at lower filler concentration. But as the concentration increased, there was a tendency for the nanofillers to agglomerate, which resulted in a reduction in mechanical properties.

Keywords: poly(butylene adipate-co-terephthalate); bionanocomposites; crystallization; morphology; tensile properties

1. Introduction

Biodegradable plastics play a vital role in today's world and have been a subject of interest to many researchers because they are cheap, renewable, easy to produce and eco-friendly. They can easily be degraded by biological agents such as algae, fungi and bacteria [1–5]. The modification of biodegradable polymer without affecting its biodegradability is of great importance to compete with the non-biodegradable polymers. This will help to reduce the pollution caused by non-biodegradable materials [6,7]. However, biodegradable polymers cannot replace any of the non-biodegradable engineering polymers because of their poor thermo-mechanical properties. Therefore, researchers have come up with copolymerizing the polymers to develop biodegradable polymers having combination of properties that complement each other [8]. One such potential copolymer is poly(butylene adipate-co-terephthalate) (PBAT), which is a copolymer of adipic acid, 1,4-butanediol and dimethyl terephthalate. PBAT is a fully biodegradable polymer capable of degrading up to 90% in just 80 days and is said to be a successful alternative for low density polyethylene (LDPE) in applications such as cling wrap for food packaging, plastic grow bags etc. [9–12]. Recently, researchers are working on replacing polyethylene mulching films used in the agricultural applications for weed control, soil moisture conservation, and temperature regulations for crops production with PBAT to reduce the environmental issues [13,14].

Studies on the replacement of carbon/glass fibers with natural fibers as reinforcement in composite material have opened up many industrial possibilities [15,16]. Natural fibers are biodegradable, light weight and cost effective. However, they have relatively high moisture sorption and poor compatibility with polymer matrix [16,17,18]. But, there are a lot of studies to control the compatibility issues with the aid of surface modifications by chemical treatments [19–22]. Among the most widely used natural fibers, hemp is one of the strongest and stiffest natural fibers. Its high specific strength, low density, eco-friendliness and low cost of production make it the best choice for developing advanced composites [23,24,25]. However, hydrophilic nature of hemp and hydrophobic nature of the polymer matrix will lead to incompatibility and thereby reduce the interfacial adhesion between the fiber and the matrix [16].

The research on PBAT composites is limited due to its low thermal stability and mechanical properties. It is usually blended with PLA, PHBV and other biopolymers to attain higher strength [25,26,27]. Dufresene et al. [28] investigated the possibility of using torrefied coffee grounds as a reinforcement for PBAT for food packaging applications with the aim to reduce the cost of PBAT composites. They observed good improvement in hydrophobicity and thermo-mechanical properties for the PBAT composites. The study of Mohanty and Nayak [29] on nanocomposites blown films based on PBAT and layered silicate revealed good improvements in tensile modulus, thermal stability and *Tg* with enhanced rate of biodegradation for the nanocomposite hybrids. Fukushima et al. [30] developed series of clay modified PBAT nanocomposites, with modified and unmodified montmorillonites, fluoro-hectorites, and unmodified sepiolites. They observed good improvement in hardness and modulus for the PBAT composites. Alkali treatment and silane functionalization on the hemp fibers and its reinforcement effect in unsaturated polyester [31] and polypropylene [32] were also reported. A good improvement in thermo-mechanical properties was reported for the chemically treated hemp reinforced polymer composites [31,32,33].

In the present work, morphology, tensile properties, viscoelasticity, thermal stability, melting, crystallization, density, and water absorption of bionanocomposites based on PBAT and different

amounts of modified and unmodified hemp fibers, carbon nanofibers (CNF) and silver nanoparticles (Ag-NPs) in PBAT matrix were studied. The hemp fibers were modified by silane after the surface treatment of the fibers with NaOH solution. CNF and Ag-NPs nanoparticles are used as nanofillers in PBAT to study the effect of nanofillers on the mechanical and thermal properties of the composites. Further, Ag-NPs based composites can be used for biomedical applications [34,35].

2. Materials and Method

2.1. Materials

Poly(butylene adipate-co-terephthalate) pellets with density of 1.25–1.27 g/cm^3, melting point of 110–120 °C and transparency of 82%, supplied by M/s BASF Japan Ltd. under the trade name Ecoflex-F BX 7011-BASF, was used as base matrix. PBAT consisted of 50 mol% of butanediol, 22 mol% of adipic acid and 28 mol% of terephthalic acid. Fully graphitic, Pyrograf III, vapour grown carbon nanofiber (trade name: PR-24-XT-HHT) with an average diameter of 100 nm and length between 50 and 200 nm was procured from Pyrograf Products. The silane used for the surface modification was bis(3-(triethoxysilyl)propyl)tetrasulfide (Si69 coupling agent). Silver nanoparticles were prepared in the Natural Composite Research lab of King Mongkut's University of Technology, North Bangkok.

2.2. Silane Functionalization of Hemp Fibers

The hemp fibers are first surface treated by alkylation, i.e., the fibers are immersed in 1% NaOH solution (10 g/L of NaOH in ethanol) and kept in an air oven for 2 h at 78 °C. It is then washed with ethanol followed by water and kept overnight at 60 °C. Meanwhile, 0.6% of Si69 in ethanol–water mixture in the ratio of 6:4 is mixed and allowed to stand for 1 h. Acetic acid is added to maintain the pH of the solution to 4. The surface treated hemp fibers were then immersed in the solution and retained in it for 1.5 h. The solution is drained out and air dried in an air oven for half an hour followed by overnight drying at 60 °C. The fibers are then grinded and sieved using an 80 mesh sieve.

2.3. Preparation of PBAT Bio-nanocomposites

PBAT composites were prepared by melt-mixing using charneotut (CT) internal mixer, Thailand. The mixing was done for 8 min at 140 °C with a rotor speed of 40 rpm. Firstly, PBAT was dried in an air oven for 18 h at 60 °C and sealed in a tight zip lock to avoid moisture. The concentrations of hemp and Si-hemp used for the preparation of composites were 2, 5, 10, 20 wt% and the concentrations of CNF and Ag-NPs were 0.05, 0.5, 1 wt% and 50, 100, 200 ppm respectively. The fillers were added after melting PBAT for 2 min followed by 6 min mixing for uniform distribution of the fillers in the matrix. The resulting composites were cut into small pieces and injection molded in a DSM Xplore 12 CC micro injection molding machine at 140 °C to prepare the test specimens for tensile testing and dynamic mechanical analysis as per relevant ISO standards.

2.4. Characterization

2.4.1. Density

The density of the samples was measured using an Alfa Mirage electronic densimeter MDS 300 by immersion at room temperature in distilled water following the ASTM D792 standard [36].

2.4.2. Morphology

Morphology of the composites was analyzed using scanning electron microscope (Hitachi), Model S-3400N. The samples for the SEM analysis were cryogenically broken by dipping in liquid nitrogen and the fracture surface is exposed to gold coating.

2.4.3. Mechanical Properties

The tensile properties of the samples were determined using a universal testing machine (Shimadzu model AGI) with a load cell of 10 kN, at a cross head speed of 50 mm/min. The Dumbbell shaped samples with dimensions 75 × 5 × 2 mm^3 were used for tensile testing according to ISO 527 standards. The samples for testing were injection molded using a 12 CC injection molding machine. The gauge length between the jaws was set to 55 mm at the start of testing.

2.4.4. Water Absorption

The hydrophilic nature of hemp fibers is a major problem for making composites. Hence, it is very relevant to detect water absorption behavior of chemically modified hemp fibers in the composites and to compare it to unmodified hemp sample. For water sorption, rectangular specimens of size 10 × 10 × 2 mm^3 were used. The samples were first dried overnight at 60 °C to remove any traces of moisture content and immediately weighed for the dry weight. The samples were then fully dipped in water at room temperature. At different time interval, the samples were removed, wiped with filter paper to remove surface water, and weighed with an analytical balance until the increase in weight of water attains equilibrium.

2.4.5. Melting and Crystallization

The melting and crystallization behavior of virgin PBAT and its composites was studied using Mettler Toledo 822e differential scanning calorimeter (DSC). Approximately 6–7 mg of sample was placed into a ceramic pan in a dry nitrogen atmosphere with a controlled nitrogen flow rate of 20 mL/min. The sample was initially scanned from −100 to 200 °C at a heating rate of 10 K/min and held at 200 °C for 5 min to erase previous thermal history, followed by cooling at 10 K/min and then it is rescanned from −100 to 200 °C.

2.4.6. Thermal Stability

The thermal stability of virgin PBAT and its composites was determined using Perkin Elmer STA 6000 TG/DTA instrument. Samples weighing 6–7 mg were scanned from 50 to 600 °C at a heating rate of 10 K/min in nitrogen atmosphere. Degradation temperatures of the samples with their corresponding weight loss were noted.

2.4.7. Viscoelasticity

The storage modulus of the samples was determined by tension mode using Mettler Toledo DMA/SDTA861^e, at a frequency of 0.1 Hz and heating rate of 10 K/min using specimens of dimensions 33 × 5 × 2 mm^3 in the temperature range of −50 to 150 °C.

3. Results and Discussion

3.1. Morphology

Morphology of different nanocomposites of PBAT is shown in Figure 1. Figure 1a shows the SEM micrograph of virgin PBAT. Figures 1b and 1c show the SEM micrographs of untreated and silane treated hemp fiber reinforced composites, respectively. Note that both untreated and silane treated hemp fibers are pulled out from the PBAT matrix. Figures 1d and 1e show the SEM micrographs of untreated and treated fibers. The diameter of the fiber is reduced from ca.40 to 30 μm for the treated fibers. This is due to the removal of pellicle layers of membrane around the fiber from the fiber surface as a result of the NaOH treatment. This layer may contain pectin, lignin and other impurities. After the treatment, the surface become free from pectin and lignin and is coated with silane. Interestingly, unlike the unmodified fiber, the surface of the modified hemp fiber is smooth probably due to the deposition of the silane layer over the surface. A similar result was obtained with henequen fibers by Gonzalez et al. [37], where the silane was effectively deposited on the fiber surface after the treatment.

Figures 1f and 1g show the SEM micrographs of CNF and Ag-NPs nanocomposites, respectively. In the CNF composites, the fibers show aggregation tendency due to van der Waals forces existing between them. CNF tend to form small globules as clusters showing the poor wettability of the fibers with matrix. It is very clear from the micrographs that the cracks are happening in front of the clusters due to stress concentrations in those regions. This may result in lower mechanical properties of the composites. Similarly, Ag-NPs particles aggregate because of the filler-filler interaction.

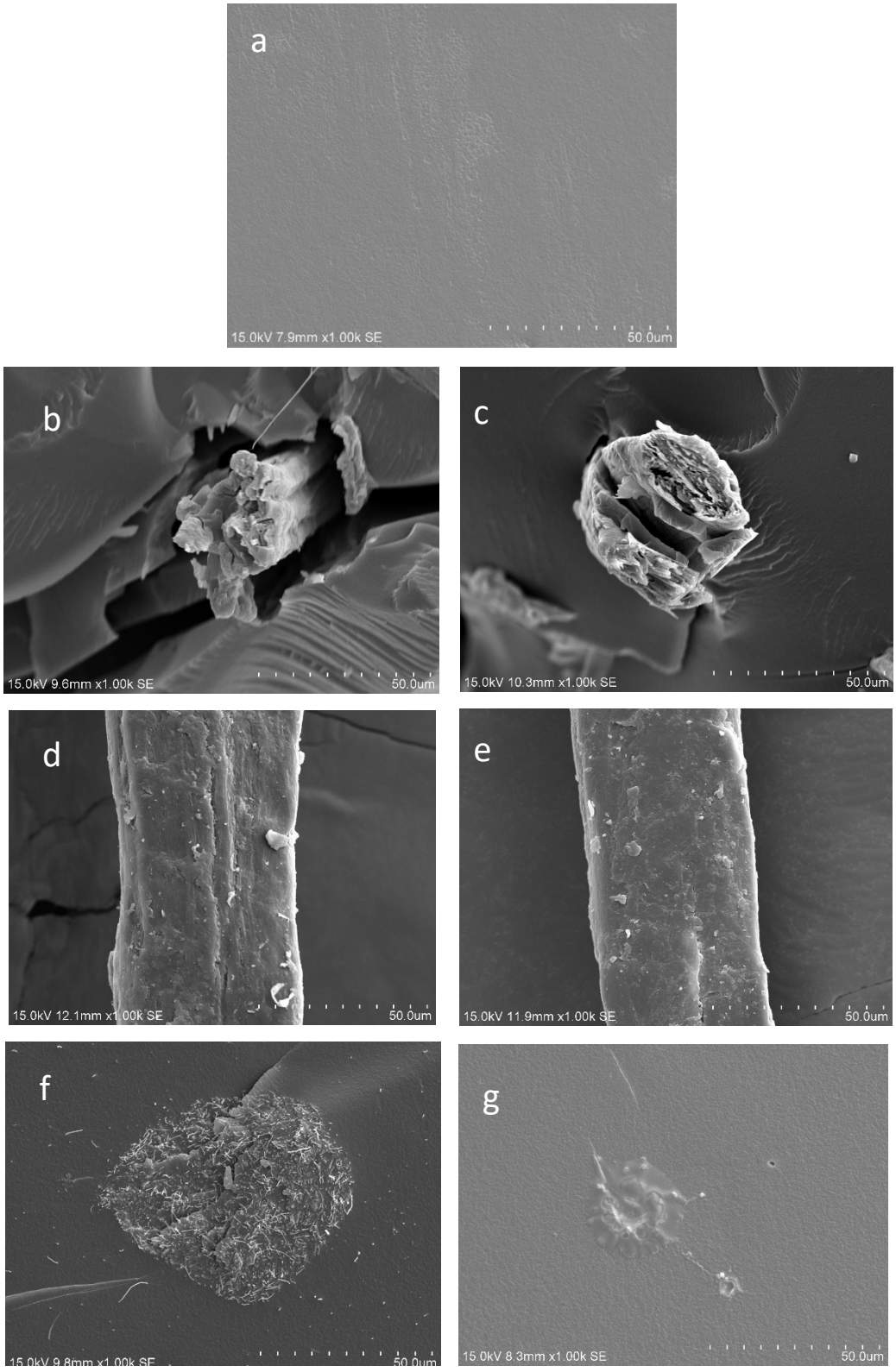

Figure 1. SEM micrographs of the PBAT composites: (a) neat PBAT, (b) PBAT/hemp, (c) PBAT/Sihemp, (d) unmodified hemp, (e) modified hemp, (f) PBAT/CNF, (g) PBAT/Ag-NPs.

3.2. Density

Figure 2 shows the density values of virgin PBAT and its nanobiocomposites. It is important to add that density plays a vital role in determining the properties of light weight composites. For many applications, light weight composites are preferred over conventional composites due to their weight savings. Irrespective of standard deviation, both hemp and Sihemp reinforced composites showed a decrease in density as the concentration of the filler is increased. Surprisingly, the density of the composites is much lower than that of neat PBAT. It is expected not to have too much variation in densities of the samples when the fiber is added, as the density of PBAT (1.16 g/cm^3) and density of hemp (unmodified 1.25 g/cm^3, silane modified 1.17 g/cm^3) are very close to each other [38]. Nevertheless, the decrease in the density of the polymer composites with increasing fiber content may be due to the generation of voids and/or cavities between the fiber and the matrix. However, the void gap between the filler and the matrix may be slightly reduced with the silane modification and hence, the density is slightly greater for silane treated hemp reinforced composites. These results are in agreement with findings of Suardana et al. [39] for PP/hemp matrix, where silane was effectively deposited on the fiber surface.

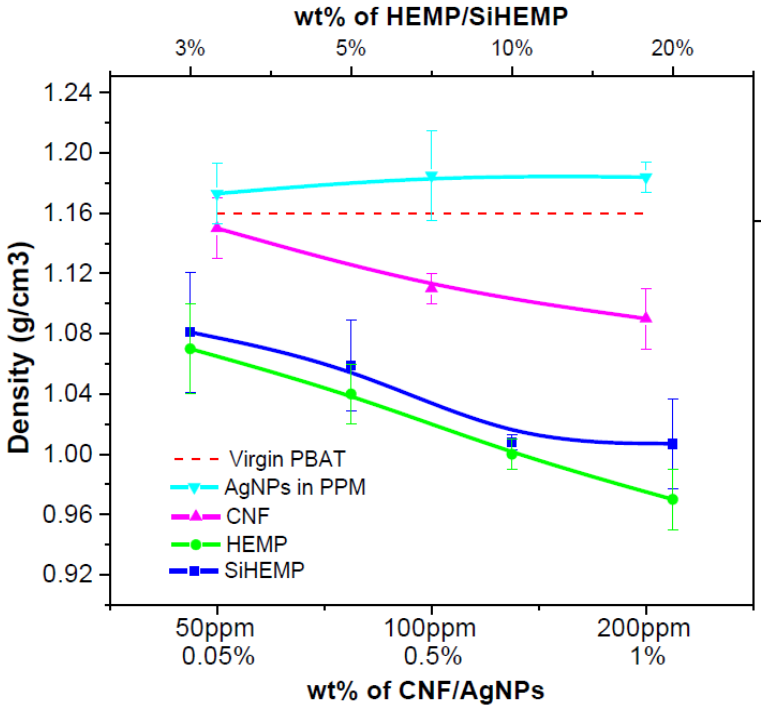

Figure 2. Variation of density with respect to concentration of nanofillers in PBAT composites.

It should be noted that the density of CNF (density of CNF: 0.02–0.05 g/cm^3) filled PBAT is close to that of neat PBAT. This is due to the flocculation of the fibers in the matrix due to poor wettability. However, the density of Ag-NPs based composites at all concentrations shows slightly higher values than neat PBAT may be due to the high density (1.2–1.3 g/cm^3) of Ag-NPs. It may also due to the close packing of silver nanoparticles in the PBAT matrix [39].

3.3. Mechanical Properties

Figures 3a–d show the variations in tensile strength (TS), tensile modulus (TM), tensile elongation (TE) and tensile toughness (TT) as a function of filler concentration. From the figures, it can be seen that both TS and TM of the samples increased with increasing concentration of unmodified and modified hemp. The TS of the composites with modified hemp increased by ca. 45% compared to ca.16% for that with the unmodified hemp. Similarly, TM of composites with modified hemp increased by ca. 334% compared to ca. 277% for that with the unmodified hemp. This is due to the fact that silane functionalization improves the fiber surface adhesion to the PBAT matrix by improving the wettability of the fiber surface and thus enhances the stress transfer between the fiber and matrix [40]. Furthermore, the surface modification reduces the hydrophilic nature of the fiber, making it more compatible with the hydrophobic matrix. This is evident from the water absorption studies; where the surface modification of hemp with silane improves the water absorption resistance. Contrary to this, TE and TT decreased with the increase in concentration of filler due to the reinforcement imparted by the fiber on the PBAT matrix [41].

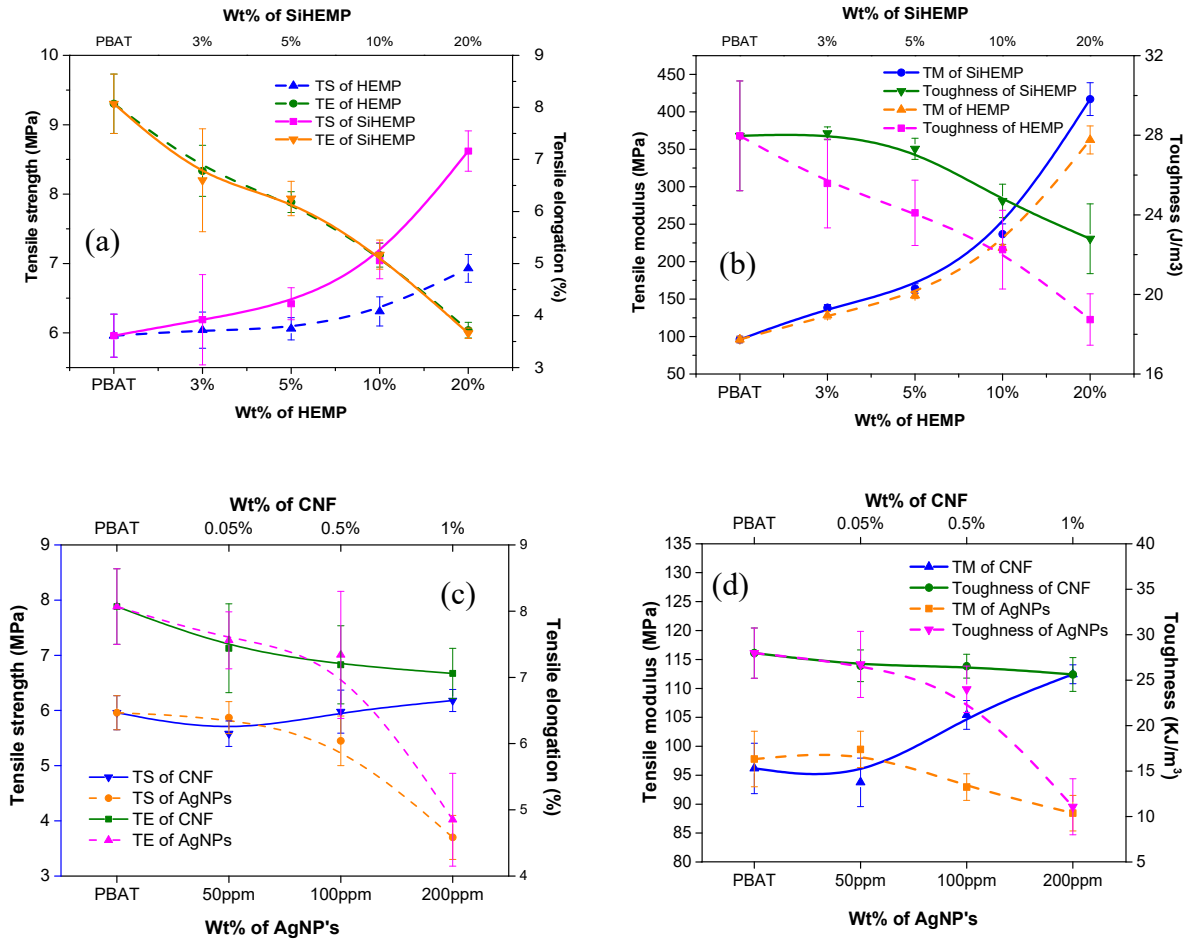

Figure 3. Tensile properties of neat PBAT and its composites (a) TS and TE of hemp and Sihemp, (b) TM and TT of hemp and Sihemp, (c) TS and TE of Ag-NPs and CNF, (d) TM and toughness of Ag-NPs and CNF.

On the other hand, CNF reinforced PBAT shows only a marginal improvement in TM (ca. 17%) and TS (ca. 4%). The toughness and elongation of the samples remain almost unchanged. This may be due to the poor wettability of CNF leading to the formation of aggregates in the PBAT matrix. This reduces the contact between the matrix and filler, which in turn diminishes the stress transfer from matrix to the fibers. All the cracks are developed in clusters of CNF. It is also interesting to note that although the tensile properties of Ag-NPs reinforced composites remain almost unaffected at lower concentrations, at higher concentrations, these properties decreased due to the higher energy of filler-filler interaction rather than filler-polymer interaction.

3.4. Water Absorption

The water uptake behavior of PBAT and its composites is shown in the Figure 4. From Figure 4, it is obvious that CNF/PBAT and Ag-NPs/PBAT composites absorbed much less water compared to hemp fiber reinforced composites. This is due to the hydrophobic nature of CNF and Ag-NPs. According to Das et al. [42], the three main regions where the water contents are observed in a natural fiber reinforced composites are cell wall, lumen, and voids between the matrix and fiber. The increased water absorption rate was noticed in hemp fiber reinforced PBAT composites mainly due to the hydrophilicity of the fiber and numerous porous tubular structures associated with lignocellulosic fibers [43]. Initially, all the natural fiber composites show tremendous increase in the water absorption but, as the immersion time of the samples increased, the absorption reached a plateau suggesting that the samples attain saturation point.

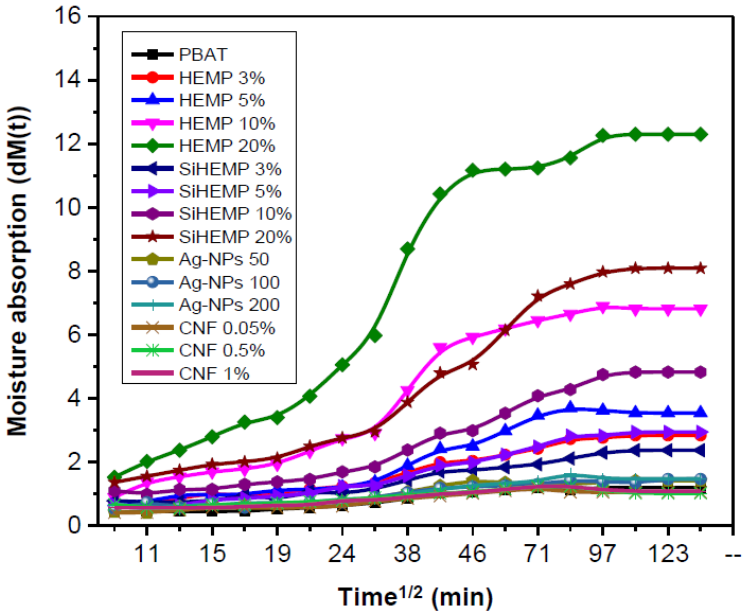

Figure 4. Moisture uptake vs $\sqrt{t}$ at room temperature of PBAT composites.

The diffusion properties of composites were evaluated by weight gain measurements of pre-dried specimen immersed in water and by considering the slope of the first part of the weight gain curve versus square root of time (t), using the following equation [44]. The coefficient of diffusion (D) defined as the slope of the normalized mass uptake against $\sqrt{t}$ and has the form:

$$D = \pi \left(\frac{kh}{4Mm}\right)^2 \quad (1)$$

where, k is the initial slope of a plot of weight gain at time t $M_{(t)}$ versus $t^{1/2}$, M_m is the maximum weight gain and h is the thickness of the composites. The Initial slope of the plot, saturation moisture (M_m) and coefficient of diffusion (D) calculated from equation 1 are given in Table 1.

Table 1. Water diffusion parameters of PBAT composites.

Samples	Initial slope of the plot (k) M_t vs $t^{1/2}$	Saturation moisture uptake M_m (%)	Diffusion coefficient D ($\times 10^{-4}$) (m^2/min)
PBAT	0.00973	1.193	0.587
hemp 3%	0.03196	2.834	1.12
hemp 5%	0.05027	3.538	1.78
hemp 10%	0.11524	6.812	2.53
hemp 20%	0.26339	12.297	4.05
Sihemp 3%	0.02677	2.367	1.13
Sihemp 5%	0.03423	2.942	1.19
Sihemp 10%	0.06364	4.824	1.54
Sihemp 20%	0.12822	8.085	2.22
Ag-NPs 50	0.01904	1.409	1.61
Ag-NPs 100	0.01854	1.463	1.42
Ag-NPs 200	0.01688	1.472	1.16
CNF 0.05%	0.0136	1.049	1.48
CNF 0.5%	0.01377	1.015	1.63
CNF 1%	0.01532	1.077	1.79

Table 1 shows that the water diffusion is higher for unmodified fiber reinforced composites because of their higher cellulosic content. However, silane functionalized hemp fiber reinforced composites show lower D values because silane acts as a hydrophobic barrier and reduces the rate of water absorption. This shows that silane functionalization improves the adhesion and reduces the moisture absorption in the fiber that may lead to better mechanical properties [45,46].

For CNF based nanocomposites, there is an increase in initial slope k and D suggesting an increase in overall water uptake. Similarly, Ag-NPs based nanocomposites show an increase in initial slope k, D and moisture uptake compared to PBAT. This is due to void spaces between the nanoparticles and matrix generated due to particle agglomeration. Interestingly, increasing concentration of Ag-NPs decreases the D value but increases the overall water uptake.

3.5. Dynamic Mechanical Analysis

Storage modulus of PBAT composites as a function of temperature are shown in Figure 5. From the figure it is evident that the stiffness of the composites increases as the fiber content increases. The increase in stiffness is maximum for the silane functionalized hemp in the whole range of the temperature, due to its better reinforcement ability in PBAT matrix. The better reinforcement restricts the chain mobility of the polymer chain which leads to a decrease in the flexibility and

increase in stiffness. At room temperature, the maximum storage modulus was exhibited by Sihemp fibers reinforced PBAT composites and minimum by Ag-NPs reinforced composites. Similar results were reported by Chatterjee et al. [39].

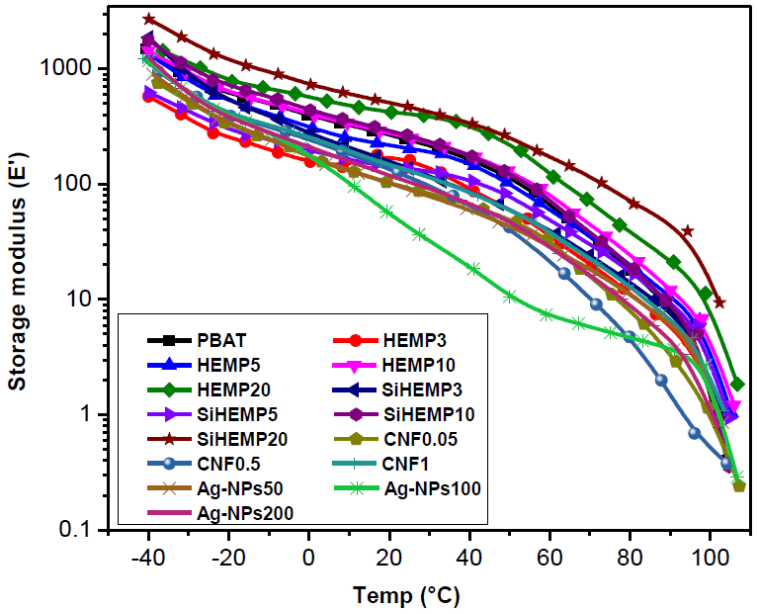

Figure 5. Storage modulus vs. temperature curves of the PBAT composites.

3.6. Thermogravimetric Analysis

Thermal stability of the PBAT and its composites in nitrogen atmosphere was studied using TGA. The TGA and DTA curves are shown in Figures 6a−b. Initial decomposition temperature (T_i), maximum decomposition temperature (T_{max}), and final decomposition temperature (T_f) obtained from the thermograms are presented in Table 2. It is evident from the figures and table that the initial and final degradation temperatures of PBAT decrease with the increase in the concentration of hemp and Sihemp showing deterioration in the thermal stability of the composites. Note that hemp is less thermally stable than PBAT. However, the thermal stability of Sihemp is higher than the hemp composites. The higher stability of Sihemp composites is due to the silane functionalization of hemp. Mwaikambu and Bisanda [47] studied alkalization and acetylation treatments of hemp fibers and reported that thermal stability was increased upon treatment. Furthermore, Beckermann and Pickering [48] reported that NaOH treatment removed all the lignin, pectin, hemicelluloses etc and increased the thermal stability. Moreover, silane functionalization would further increase the stability of the system as a result of better interlocking of the treated fibers with the matrix as seen in the SEM images.

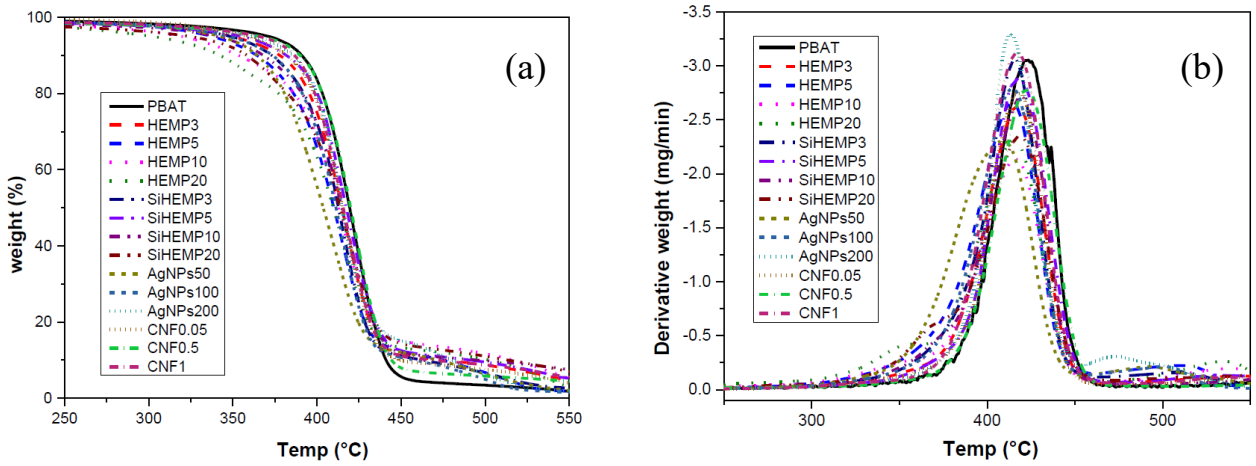

Figure 6. (a) TGA curves of PBAT composites, (b) DTG curves of PBAT composites.

Table 2. Thermal degradation parameters of PBAT composites.

Samples	T_i (°C)	T_f (°C)	T_{max} (°C)
PBAT	396.34	440.83	422.86
hemp3	388.31	436.65	412.21
hemp5	376.79	429.2	413.97
hemp10	374.06	426.65	416.92
hemp20	371.86	421.39	415.07
Sihemp3	393.68	442.03	416.12
Sihemp5	392.84	436.34	417.21
Sihemp10	385.95	436.65	418.84
Sihemp20	383.65	436.65	419.12
Ag-NPs 50	368.67	422.87	408.55
Ag-NPs 100	383.68	432.03	413.97
Ag-NPs 200	399.83	435.63	412.77
CNF0.05	387.56	432.41	417.27
CNF0.5	396.73	440.39	422.17
CNF1	392.84	436.65	417.27

In the case of Ag-NPs reinforced composites, thermal degradation parameters such as T_i, T_{max}, and T_f show no appreciable change, suggesting that the presence of Ag-NPs have little impact on the thermal stability of the PBAT. However, Ag-NPs are supposed to exhibit a shielding effect on the matrix to slow the rate of mass loss of decomposition product [49], which is not reflected in our studies. Similarly, CNF reinforced composites show slight changes in thermal stability of the PBAT matrix probably due to the very small amount of CNF in the composites.

3.7. Differential Scanning Calorimetry

DSC heating and cooling curves of PBAT based composites are shown in the Figures 7a–b, respectively. The DSC heating curves show three different widely spaced distinct melting

endotherms for PBAT in all the composites. The melting temperatures are in the range 53−56 °C for 1st transition, 90−95 °C for 2nd transition and 129−135 °C for 3rd transition. Even though such multiple thermograms are common among semicrystalline polymers, the distinct and widely spaced thermograms are seldom reported in literature. The most probable reasons for such behavior could be the continuous melting and recrystallization processes [50,51]. Another reason could be the thermal history of the sample during the processing, where sample was suddenly cooled after processing. This may lead to lamellar formations of crystals of different sizes that show different degrees of melting temperatures.

On the other hand, broad crystallization peaks are observed for PBAT and PBAT based composites (Figure 7b). From Table 3 it is clear that the crystallization temperatures of the composites increase by the addition of fillers. This is because of the nucleating action of the fillers in the PBAT matrix which thereby increases the temperature of crystallization during cooling.

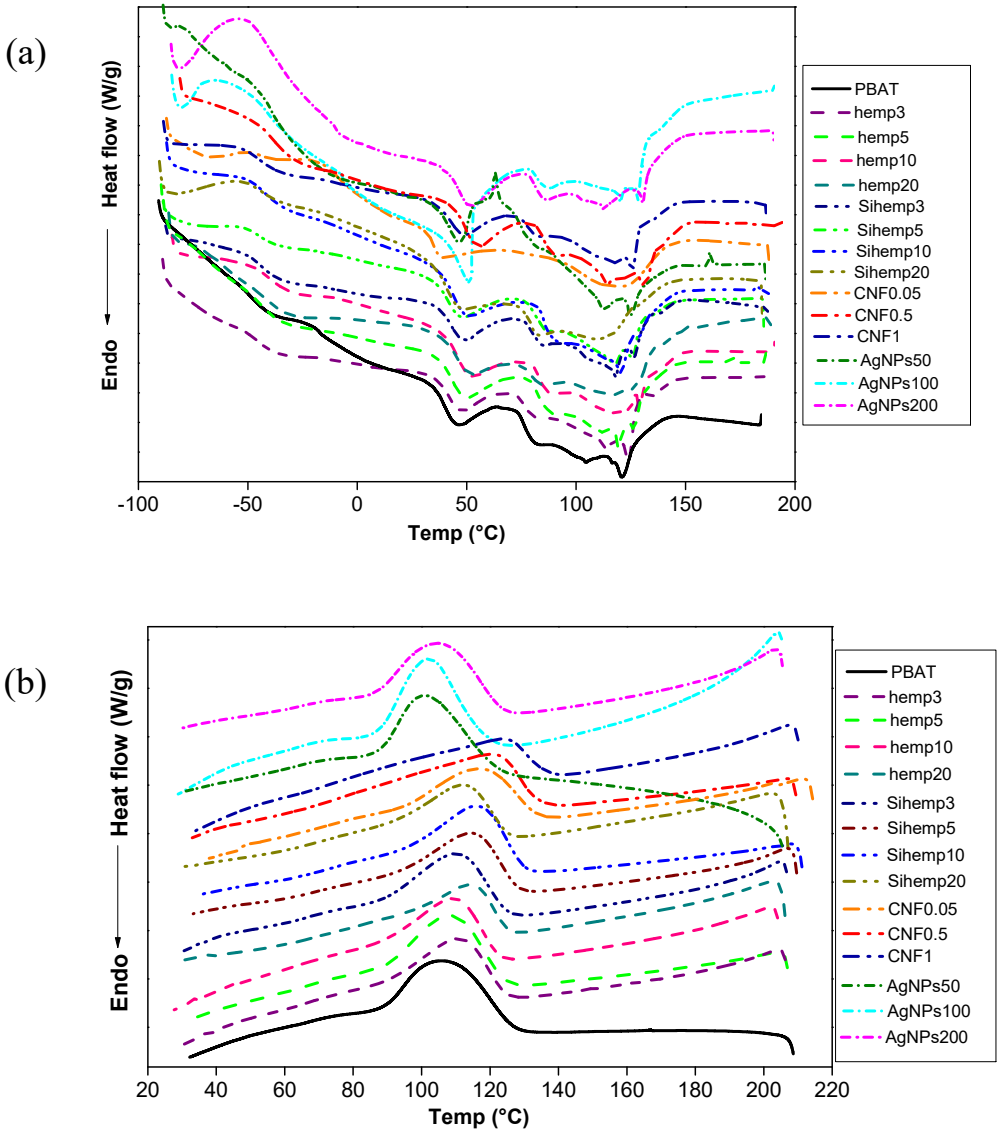

Figure 7. (a) Heating curves showing the melting temperatures of PBAT composites, (b) Cooling curves showing the crystallization temperatures of PBAT composites.

The highest value of crystallization temperature is obtained for CNF based composites, where the crystallization temperature increases from 101.34 °C for virgin PBAT to 116.8 °C for 1% CNF filled PBAT. It should be noted that as hemp is functionalized with silane, the crystallization temperature is comparatively less, suggesting good adhesion between the silane functionalized hemp and PBAT over the PBAT/hemp composites. On the other hand, the enthalpy of crystallization (ΔH_c) of PBAT decreases by the addition of fillers. Note that T_g of the composites were approximately stable with minor fluctuations.

Table 3. Glass transition, crystallization and melting temperatures of PBAT and its composites.

Samples	T_g (°C)	T_c (°C)	ΔH_c (Jg^{-1})	T_m(°C)		
				1	2	3
PBAT	−47.01	101.34	12.94	55.18	91.65	133.42
hemp3	−47.11	107.66	10.4	55.08	89.37	134.55
hemp5	−45	104.53	11.75	56.68	97.81	129.42
hemp10	−47.95	107.84	11.93	54.89	92.02	130.65
hemp20	−59.88	110.47	8.76	56.22	90.53	134
Sihemp3	−49.4	106.33	11.71	54.4	91.05	127.17
Sihemp5	−47.11	107.65	10.76	55.74	95.22	129.55
Sihemp10	−48.37	108.03	12.09	55.53	97.32	128.77
Sihemp20	−48.99	108	8.74	55.72	92.85	128.83
Ag-NPs 50	−41.41	97.81	12.35	53.52	-	135.08
Ag-NPs 100	−53.54	100.19	12.88	55.17	-	134.68
Ag-NPs 200	−49.47	114.37	9.2	54.69	90.33	134.77
CNF 0.05	−48.73	105.61	9.2	44.44	-	131.23
CNF 0.5	−51.16	114.6	8.31	54.69	90.33	133.44
CNF 1	−50.12	116.8	5.16	55.75	91.24	136.02

4. Conclusions

The present research deals with the investigation of physical properties, thermo-mechanical properties and the morphology of PBAT and its composites with different weight percentage of hemp, Sihemp, CNF and Ag-NPs. The density study reveals that the densities of composite are considerably reduced upon addition of hemp and Sihemp fibers, signifying the development of light weight composite materials.SEM analysis shows better interaction between Sihemp fibers and PBAT matrix over hemp and PBAT, which is reflected in tensile properties of the composites. The diffusion coefficient and maximum water absorption of the composites are reduced for silane functionalized hemp reinforced composites. Hence, the silane functionalization helps in reducing the water absorption of the fiber reinforced composites for the use in moisture conditions or exterior automotive applications and for food packaging containers as hemp has some antibacterial properties. The thermal stability of PBAT is retained in fiber reinforced composites.CNF based composites show no significant improvement in the properties as the poor dispersion of CNF in PBAT matrix, due to poor wettability. The density of Ag-NPs is slightly higher than the neat PBAT and the mechanical properties are inferior to neat PBAT at higher concentrations because of the poor interfacial interaction between the matrix and filler. Thermo-mechanical properties of Ag-NPs

reinforced composites are retained at lower filler concentration. Thus, combination of Ag-NPs/Sihemp/PBAT hybrid composites could be beneficial for developing biocompatible composites and biodegradable hybrids with good antibacterial properties.

Acknowledgement

The authors would like to acknowledge the Sirindhorn international Thai German graduation school, King Mongkut's University of Technology North Bangkok for funding this project and during the short term visit to Thailand under the grant agreement KMUTNB-61-KNOW-001. J P acknowledges the Department of Science and Technology, Government of India, for financial support under an Innovation in Science Pursuit for Inspired Research (INSPIRE) Faculty Award (contract grant number IFA-CH-16).

Conflict of Interest

All authors declare on conflict of interest in this paper.

References

1. Abraham JD, Kost J, Wiseman D (1998) *Handbook of biodegradable polymers*, CRC Press.
2. Demirbas A (2007) Biodegradable plastics from renewable resources. *Energ Sources Part A* 29: 419–424.
3. Weng YX, Jin YJ, Meng QY, et al. (2013) Biodegradation behavior of poly(butylene adipate-co-terephthalate) (PBAT), poly(lactic acid) (PLA), and their blend under soil conditions. *Polym Test* 32: 918–926.
4. Mondal D, Bhowmick B, Mollick MR, et al. (2014) Antimicrobial activity and biodegradation behavior of poly(butylene adipate-co-terephthalate)/clay nanocomposites. *J Appl Polym Sci* 131: 40079.
5. Jiang L, Wolcott MP, Zhang J (2006) Study of Biodegradable Polylactide/Poly(butylene adipate-co-terephthalate) Blends. *Biomacromolecules* 7: 199–207.
6. Comanita ED, Hlihor RM, Ghinea C, et al. (2016) Occurrence of plastic waste in the environment: Ecological and health risks. *Environ Eng Manag J* 15: 675–685.
7. Verma R, Vinoda KS, Papireddy M, et al. (2016) Toxic Pollutants from Plastic Waste—A Review. *Procedia Environ Sci* 35: 701–708.
8. Genovese L, Lotti N, Gazzano M, et al. (2016) Novel biodegradable aliphatic copolyesters based on poly(butylene succinate) containing thioether-linkages for sustainable food packaging applications. *Polym Degrad Stabil* 132: 191–201.
9. Peres AM, Pires RR, Oréfice RL (2016) Evaluation of the effect of reprocessing on the structure and properties of low density polyethylene/thermoplastic starch blends. *Carbohyd Polym* 136: 210–215.
10. Debeaufort F, Gallo JAQ, Voilley A (1998) Edible Films and Coatings: Tomorrow's Packagings: A Review. *Crit Rev Food Sci* 38: 299–313.

11. Arvanitoyannis I, Biliaderis CG, Ogawa H, et al. (1998) Biodegradable films made from low density polyethylene (LDPE), rice starch and potato starch for food packaging application: Part I. *Carbohyd Polym* 36: 89–104.
12. Tharanathan RN (2003) Biodegradable films and composite coatings: past, present and future. *Trends Food Sci Tech* 14: 71–78.
13. Kushwaha PK, Kumar R (2010) Studies on Water Absorption of Bamboo-Polyester Composites: Effect of Silane Treatment of Mercerized Bamboo. *Polym-Plast Technol* 49: 45–52.
14. Touchaleaume F, Closas LM, Coussy HA, et al. (2016) Performance and environmental impact of biodegradable polymers as agricultural mulching films. *Chemosphere* 144: 433–439.
15. Saba N, Jawaid M, Alothman OY, et al. (2016) A review on dynamic mechanical properties of natural fibre reinforced polymer composites. *Constr Build Mater* 106: 149–159.
16. Balakrishnan P, John MJ, Pothen L, et al. (2016) Natural fibre and polymer matrix composites and their applications in aerospace engineering, In: Rana S, Fangueiro R, *Advanced Composite Materials for Aerospace Engineering: Processing, Properties and Applications*, 365–383.
17. George M, Chae M, Bressler DC (2016) Composite materials with bast fibres: Structural, technical, and environmental properties. *Prog Mater Sci* 83: 1–23.
18. Džalto J, Medina LA, Mitschang P (2014) Volumetric interaction and material characterization of flax/furan biocomposites. *KMUTNB: IJAST* 7: 11–21.
19. John MJ, Anandjiwala RD (2008) Recent developments in chemical modification and characterization of natural fiber-reinforced composites. *Polym Composite* 29: 187–207.
20. Li X, Tabil LG, Panigrahi S (2007) Chemical treatments of natural fiber for use in natural fiber-reinforced composites: a review. *J Polym Environ* 15: 25–33.
21. Mwaikambo LY, Ansell MP (2002) Chemical modification of hemp, sisal, jute, and kapok fibers by alkalization. *J Appl Polym Sci* 84: 2222–2234.
22. Orue A, Jauregi A, Peña-Rodriguez C, et al. (2015) The effect of surface modifications on sisal fiber properties and sisal/poly (lactic acid) interface adhesion. *Compos Part B-Eng* 73: 132–138.
23. Shahzad A (2012) Hemp fiber and its composites—a review. *J Compos Mater* 46: 973–986.
24. Karger-Kocsis J, Siengchin S (2014) Single-Polymer Composites: Concepts, Realization and Outlook: Review. *KMUTNB: IJAST* 7: 1–9.
25. Zolali AM, Favis BD (2017) Partial to complete wetting transitions in immiscible ternary blends with PLA: the influence of interfacial confinement. *Soft Matter* 13: 2844–2856.
26. Nofar M, Tabatabaei A, Sojoudiasli H, et al. (2017) Mechanical and bead foaming behavior of PLA-PBAT and PLA-PBSA blends with different morphologies. *Eur Polym J* 90: 231–244.
27. Wu N, Zhang H (2017) Mechanical properties and phase morphology of super-tough PLA/PBAT/EMA-GMA multicomponent blends. *Mater Lett* 192: 17–20.
28. Moustafa H, Guizani C, Dupont C, et al. (2017) Utilization of Torrefied Coffee Grounds as Reinforcing Agent To Produce High-Quality Biodegradable PBAT Composites for Food Packaging Applications. *ACS Sustain Chem Eng* 5: 1906–1916.
29. Mohanty S, Nayak SK (2010) Biodegradable nanocomposites of poly(butylene adipate-co-terephthalate) (PBAT) with organically modified nanoclays. *Int J Plast Technol* 14: 192–212.
30. Fukushima K, Wu MH, Bocchini S, et al. (2012) PBAT based nanocomposites for medical and industrial applications. *Mater Sci Eng C-Mater Biol Appl* 32: 1331–1351.

31. Dhakal HN, Zhang ZY, Bennett N (2012) Influence of fibre treatment and glass fibre hybridization on thermal degradation and surface energy characteristics of hemp/unsaturated polyester composites. *Compos Part B-Eng* 43: 2757–2761.
32. Panaitescu DM, Nicolae CA, Vuluga Z, et al. (2016) Influence of hemp fibers with modified surface on polypropylene composites. *J Ind Eng Chem* 37: 137–146.
33. Phongam N, Dangtungee R, Siengchin S (2015) Comparative studies on the mechanical properties of nonwoven- and woven-flax-fiber-reinforced poly(butylene adipate-co-terephthalate)-based composite laminates. *Mech Compos Mater* 51: 17–24.
34. Kim JS, Kuk E, Yu KN, et al. (2007) Antimicrobial effects of silver nanoparticles. *Nanomed-Nanotechnol* 3: 95–101.
35. Abdo HS, Khalil AK, Al-deyab SS, et al. (2013) Antibacterial effect of carbon nanofibers containing Ag nanoparticles. *Fiber Polym* 14: 1985–1992.
36. ASTM D792 (2000) Standard Test Methods for Density and Specific Gravity (Relative Density) of Plastics by Displacement.
37. Valadez-Gonzalez A, Cervantes-Uc JM, Olayob R, et al. (1999) Effect of fiber surface treatment on the fiber-matrix bond strength of natural fiber reinforced composites. *Compos Part B-Eng* 30: 309–320.
38. Suardana NPG, Piao Y, Lim JK (2011) Mechanical Properties of Hemp Fibers and Hemp/PP Composites: Effects of Chemical Surface Treatment. *Mater Phys Mech* 11: 1–8.
39. Chatterjee U, Jewrajka SK, Guha S (2009) Dispersion of functionalized silver nanoparticles in polymer matrices: Stability, characterization, and physical properties. *Polym Composite* 30: 827–834.
40. Dhakal HN, Zhang ZY, Richardson MOW (2007) Effect of water absorption on the mechanical properties of hemp fibre reinforced unsaturated polyester composites. *Compos Sci Technol* 67: 1674–1683.
41. Lin S, Guo W, Chen C, et al. (2012) Mechanical properties and morphology of biodegradablepoly(lactic acid)/poly(butylene adipate-co-terephthalate) blends compatibilized by transesterification. *Mater Design* 36: 604–608.
42. Das S, Saha AK, Choudhury PK, et al. (2000) Effect of steam pretreatment of jute fiber on dimensional stability of jute composite. *J Appl Polym Sci* 76:1652–1661.
43. Nagarajan V, Mohanty AK, Misra M (2013) Sustainable Green Composites: Value Addition to Agricultural Residues and Perennial Grasses. *ACS Sustain Chem Eng* 1: 325–333.
44. Banks WM, Dumolin F, Hayward D, et al. (1996) Nondestructive examination of composite joint structures: a correlation of water absorption and high-frequency dielectric propagation. *J Phys D-Appl Phys* 29: 233–239.
45. Wang W, Sain M, Cooper PA (2006) Study of moisture absorption in natural fibre plastic composites. *Compos Sci Technol* 66: 379–386.
46. Sreekala MS, Thomas S (2003) Effect of fibre surface treatment on water sorption characteristics of oil palm fibres. *Compos Sci Technol* 63: 861–869.
47. Mwaikambo LY, Bisanda ETN (1999) The performance of cotton-kapok fabric-polyester composites. *Polym Test* 18: 181–198.
48. Beckermann GW, Pickering KL (2008) Engineering and evaluation of hemp fiber reinforced polypropylene composites: Fibre treatment and matrix modification. *Compos Part A-Appl S* 39: 979–988.

49. Ou CF, Ho MT, Lin JR (2004) Synthesis and characterization of poly(ethylene terephthalate) nanocomposites with organoclay. *J Appl Polym Sci* 91: 140–145.
50. Tregub A, Karger-Kocsis J, Koennnecke K, et al. (1995) Deformation and Thermoelastic Behavior of Poly(aryl ether ketones). *Macromolecules* 28: 3890–3893.
51. Velikov V, Marand H (1997) Studies of the enthalpy relaxation and the "multiple melting" behavior of semicrystalline poly(arylene ether ether ketone) (PEEk). *J Therm Anal Calorim* 49: 375–383.

AIMS Press